Original Research Article

Emerging role of vitamin D₃ in alleviating intestinal structure injury caused by *Aeromonas hydrophila* in grass carp (*Ctenopharyngodon idella*)

Yao Zhang [a], Xiao-Qiu Zhou [a, b, c], Wei-Dan Jiang [a, b, c], Pei Wu [a, b, c], Yang Liu [a, b, c], Hong-Mei Ren [a, b, c], Lu Zhang [d], Hai-Feng Mi [d], Ling Tang [e], Cheng-Bo Zhong [e], Lin Feng [a, b, c, *]

[a] *Animal Nutrition Institute, Sichuan Agricultural University, Chengdu, China*
[b] *Fish Nutrition and Safety Production University Key Laboratory of Sichuan Province, Sichuan Agricultural University, Chengdu, China*
[c] *Key Laboratory for Animal Disease-Resistant Nutrition of China Ministry of Education, Sichuan Agricultural University, Chengdu, China*
[d] *Healthy Aquaculture Key Laboratory of Sichuan Province, Tongwei Co., Ltd., Chengdu, China*
[e] *Sichuan Animal Science Academy, Sichuan Animtech Feed Co., Ltd., Chengdu, China*

ARTICLE INFO

ABSTRACT

Bacterial pathogens destroy the structural integrity of functional organs in fish, leading to severe challenges in the aquaculture industry. Vitamin D₃ (VD₃) prevents bacterial infections and strengthens immune system function via vitamin D receptor (VDR). However, the correlation between VD₃/VDR and the structural integrity of functional organs remains unclarified. This study aimed to investigate the influence of VD₃ supplementation on histological characteristics, apoptosis, and tight junction characteristics in fish intestine during pathogen infection. A total of 540 healthy grass carp (257.24 ± 0.63 g) were fed different levels of VD₃ (15.2, 364.3, 782.5, 1,167.9, 1,573.8, and 1,980.1 IU/kg) for 70 d. Subsequently, fish were challenged with *Aeromonas hydrophila*, a pathogen that causes intestinal inflammation. Our present study demonstrated that optimal supplementation with VD₃ (1) alleviated intestinal structural damage, and inhibited oxidative damage by reducing levels of oxidative stress biomarkers; (2) attenuated excessive apoptosis-related death receptor and mitochondrial pathway processes in relation to p38 mitogen-activated protein kinase signaling ($P < 0.05$); (3) enhanced tight junction protein expression by inhibiting myosin light chain kinase signaling ($P < 0.05$); and (4) elevated VDR isoform expression in fish intestine ($P < 0.05$). Overall, the results demonstrated that VD₃ alleviates oxidative injury, apoptosis, and the destruction of tight junction protein under pathogenic infection, thereby strengthening pathogen defenses in the intestine. This finding supports the rationale for VD₃ intervention as an essential practice in sustainable aquaculture.

1. Introduction

Bacterial pathogens are a major constraint in aquaculture because they destroy the structural integrity of fish organs, posing severe economic and environmental challenges to the industry (Granada et al., 2016). In general, disrupted structural integrity is caused by alterations in the production of specific tight junction proteins (Berkes et al., 2003). Therefore, strategies to enhance pathogen resistance and strengthen tight junction proteins are urgently required. To this end, nutritional regulation has been implemented to alleviate the adverse effects of bacterial infection by promoting the healthy development of aquatic animals.

Vitamin D$_3$ (VD$_3$), as an essential nutrient, prevents bacterial infection and enhances the structural integrity of functional organs in mammals (Christakos et al., 2016). Previous studies of aquatic animals have revealed the key roles of VD$_3$ in growth performance, lipid metabolism, glucose homeostasis, and oxidation resistance (Li et al., 2021; Liu et al., 2021a; Wu et al., 2020). However, few studies have examined whether VD$_3$ protects the structure of functional organs during pathogen infection. Our previous study demonstrated that dietary VD$_3$ promotes growth performance and amino acid absorption in the fish intestine (Zhang et al., 2022); the function of which depends primarily on its structural integrity (Yuan et al., 2021). Fish intestines possess a delicate structure and are susceptible to the invasion of numerous pathogens, which can result in substantial losses for the aquaculture industry (Salinas and Parra, 2015). Therefore, promoting intestinal structural integrity is essential for the maintenance of animal health and for the sustainability of commercial production. VD$_3$ mediates pleiotropic effects via the vitamin D receptor (VDR), which possesses two unique isoforms in fish (VDRa and VDRb) (Craig et al., 2008) and regulates tissue barriers in mammals (Zhang et al., 2013). Nevertheless, the characteristics of VDR isoform-mediated functions and the effect of dietary VD$_3$ administration on their underlying mechanisms have yet to be investigated in fish. Therefore, exploring the relationship between VD$_3$ and intestinal structural integrity is necessary to promote and advance nutritional regulation in aquaculture.

Pathogenic infections in fish compromise the structural integrity of the intestine, leading to apoptosis (Shah et al., 2019). VD$_3$ inhibited intestinal epithelial apoptosis and maintained intestinal epithelial turnover in rats (Wang et al., 2019). In chicken jejunal tissue, VD$_3$ supplementation alleviated apoptosis levels in epithelial cells (Nong et al., 2023). Thus far, little is currently known about the link between VD$_3$ and cell apoptosis. VD$_3$ supplementation alleviated cell damage and apoptosis and promoted cell proliferation in spleen of Asian Swamp Eel (*Monopterus albus*) (Li et al., 2013). Moreover, a previous study has shown that an increased number of apoptotic cells in the small intestine were observed in VDR-deficient mice (Lu et al., 2019). However, the specific mechanism of VD$_3$ associated with VDR on cell apoptosis has not been systematically investigated in fish. Therefore, an intensive investigation into the effects of VD$_3$ on cell apoptosis in fish intestine is necessary.

Apoptosis results in the disruption of the intestinal epithelial cell barrier (Chin et al., 2006), which is regulated by tight junction proteins (Wang et al., 2015a). Tight junctions are crucial for intestinal barrier function and are composed of different junctional molecules, such as occludin and claudin (Niessen, 2007). Limited studies suggest that VD$_3$ alleviates lipopolysaccharide-induced damage of tight junctions in yellow catfish (*Pelteobagrus fulvidraco*) intestine (Liu et al., 2021b). Moreover, VDR knockout accounted for the depressed expression of occludin and zonula occludens-1 (ZO-1) in mouse cornea (Elizondo et al., 2014). In VDR-deficient mice, mRNA levels of claudin-2, -4, and -18 were reduced in the lungs (Chen et al., 2018). However, none of the study characteristics explained the possible effects of VD$_3$ allied with VDR on tight junctions in fish. Therefore, the function of VD$_3$ in tight junctions, as well as the underlying molecular mechanism, remains largely unknown and requires further study.

In the present study, we examined whether VD$_3$ can protect fish intestines from apoptosis and tight junction damage under pathogen infection. Grass carp (*Ctenopharyngodon idella*) is one of the most economically important species in China and has been introduced to over 100 countries for aquaculture (Wang et al., 2015b). In 2019, the global production of grass carp yielded over 50 million tonnes (FAO, 2020). However, the advent of high-density aquaculture in recent years has resulted in heightened susceptibility to various pathogens. Among these, *Aeromonas hydrophila* is the most frequent culprit of infections in grass carp culture, leading to substantial losses in the aquaculture industry (Zhang et al., 2023). And *A. hydrophila* exhibit multiple routes of pathogenicity with extracellular proteins such as aerolysin, lipase, and chitinase, making it ideal as an experimental bacterium (Abreu et al., 2018). Past studies have shown that *A. hydrophila* can cause severe intestinal damage in fish, including inflammatory cell infiltration and microvillus effacement in grass carp (Kong et al., 2017; Song et al., 2014) and intestinal mucus layer damage in common carp (Schroers et al., 2009). This damage makes fish intestinal mucosa less effective against subsequent pathogens. To this end, the current study is aimed to investigate, for the first time, the role of VD$_3$, VDR, and potential signaling molecules such as p38 mitogen-activated protein kinase (p38MAPK) and myosin light chain kinase (MLCK) in regulating apoptosis and tight junctions in the intestines of grass carp following infection with *A. hydrophila*. Our results highlight the role of VD$_3$–associated molecular pathways in intestinal regulation and support the rationale for nutritional intervention in aquaculture.

2. Materials and methods

2.1. Animal ethics statement

The experimental procedures followed in this study were conducted in accordance with the guidelines of the University of Sichuan Agricultural Animal Care Advisory Committee (Sichuan, China).

2.2. Diets and experimental management

The experimental diets are shown in Table S1. Soybean protein concentrate, gelatin, and casein were principally used as protein sources, and linseed and soy oils were used as lipid sources. VD$_3$ was purchased from Jindawei Co., Ltd. (Xiamen, China). Six experimental diets were prepared with VD$_3$ levels of 0 (unsupplemented control), 400, 800, 1,200, 1,600, and 2,000 IU/kg feed. After analysis, the final amounts of VD$_3$ were 15.2 (unsupplemented control; VD15.2), 364.3 (VD364.3), 782.5 (VD782.5), 1,167.9 (VD1,167.9), 1,573.8 (VD1,573.8), and 1,980.1 (VD1,980.1) IU/kg feed. All diet ingredients were mixed, compacted into pellets, and stored at −20 °C.

Fish were first acclimatized for 4 weeks in a culturing fishpond and subsequently provided with a basal diet (without VD$_3$ supplementation) for 2 weeks to reduce pre-accumulated VD$_3$ levels. Before the feeding trial, 540 grass carp (257.24 ± 0.63 g, mean ± SD) were randomly divided into 18 culture cages (140 cm × 140 cm × 140 cm) in outdoor freshwater ponds, with 30 fish per cage. The rearing cages were maintained under a natural light-dark cycle. Water quality was monitored daily and the following parameters were maintained: dissolved oxygen > 6 mg/L, water temperature 28.0 ± 2.1 °C, and pH 7.0 ± 0.2.

2.3. Challenge trial and sampling

The challenge trial with *A. hydrophila* was performed according to the method described by Xu et al. (2016). At the end of the 70-d growth period, the fish were transferred to new experimental cages and acclimatized to rearing conditions for 5 d (Tian et al., 2017). Subsequently, fish were challenged by intraperitoneal injection of 1.0 mL of 2.5 × 10^8 colony-forming units/mL of *A. hydrophila* (Zhang et al., 2023). The pathogen concentration was a non-lethal dosage sufficient to activate the immune system and,

consequently, enable the investigation of fish reactivity against a threatening disease (Luo et al., 2014). The challenge trial duration was 2 weeks. Before sampling, fish were fasted for 24 h, selected randomly, and euthanized in a benzocaine bath (50.0 mg/L) (Xu et al., 2016). Fish intestines were immediately segmented into 3 parts (proximal intestine [PI], mid-intestine [MI], and distal intestine [DI]) according to the methods of a previous study (Ni and Wang, 1999). The intestines from 6 fish per cage were preserved at −80 °C for subsequent analyses using real-time quantitative polymerase chain reaction (qPCR), biochemical assays, and Western blot analysis. Intestines from another 6 fish per cage were preserved in 4% paraformaldehyde for histological analysis.

2.4. Diet composition and biochemical assay

The approximate diet compositions were analyzed using standard methods (AOAC, 2005). Further, moisture and crude protein contents were determined using a vacuum freeze dryer (GZX-9240MBE, Boxun, Shanghai, China) and an auto Kjeldahl system (Kjeltec 8400, FOSS, Copenhagen, Denmark), respectively. Crude lipid levels were determined using the Soxhlet extraction method (AOAC, 2005). Intestine samples were homogenized in cold saline (10%, wt/vol) and centrifuged at $1,300 \times g$ at 4 °C for 15 min, after which the supernatant was collected for analysis. The methods used to analyze the antioxidant and immune parameters are listed in Table S2.

2.5. Real-time qPCR

The RNA extraction, complementary DNA transcription, and gene transcription in intestinal segments were performed according to the method described by Zhang et al. (2022). RNA extraction was performed using the RNAiso Plus kit (Takara Bio, Kusatsu, Japan) according to manufacturer instructions and treated with DNase I (Beyotime, Nanjing, China). Agarose gel electrophoresis (1%) and spectrophotometric (A_{260}/A_{280} ratio) analyses were used to confirm RNA purity and quantity, respectively. Reverse transcription of RNA was performed using a PrimeScript RT Reagent Kit (Takara Bio, Kusatsu, Japan) according to manufacturer instructions. And β-actin was used as a reference gene for normalization. The operating procedures were started with pre-heating for 5 min at 95 °C, 1 cycle running at 95 °C for 5 s and 60 °C (annealing temperature) for 30 s, and then followed with 40 cycles in the QuantStudio5 instrument (Thermo Fisher Scientific, New York, USA). The expression of all genes was calculated using the $2^{-\Delta\Delta CT}$ method (Wu et al., 2020). The primers used are listed in Table S3.

2.6. Western blot analysis

Protein extraction, gel electrophoresis, membrane transfer, blocking, antibody incubation, and quantification were performed as described in our previous study (Zhang et al., 2022). The homogenized tissue was extracted in lysis solution (radio immuno-precipitation assay lysis buffer:phenylmethylsulfonyl fluorid = 89:1) for 30 min and centrifuged at $14,000 \times g$ for 3 min at 4 °C. The supernatant was extracted and treated with $5\times$ loading buffer (Beyotime, Nanjing, China). The protein concentration of the samples was determined using a BCA kit (Beyotime, Nanjing, China) with denaturing at 96 °C for 8 min. Equal amounts of extracted protein (40 μg per lane) were separated by gel electrophoresis and transferred to polyvinylidene fluoride membranes. The membranes were blocked with bovine serum albumin (BSA; 5%) at room temperature (approximately 20 °C) for 1.5 h and incubated overnight with a primary antibody at 4 °C. The membranes were then incubated with a goat anti-rabbit horseradish peroxidase-conjugated secondary antibody for 2 h and visualized using a ChemiDo Touch Analyzer (Bio-Rad Laboratories, Hercules, CA, USA). Information regarding the antibodies used in the Western blot analysis is listed in Table S4.

2.7. Frozen sectioning, hematoxylin and eosin (H&E) staining, immunohistochemical analysis, and immunofluorescence

Frozen sections were obtained following the procedure described by Feng et al. (2016). Intestinal tissues were embedded in molds with Tissue-Tek O.C.T. Compound (Sakura Finetek Japan, Tokyo, Japan), cooled in liquid nitrogen, and stored at −80 °C. The 10-μm sections were prepared using a freezing microtome (CM1950, Leica Biosystems, Wetzlar, Germany), collected on positively charged microscope slides (188158, Liusheng, Shanghai, China), and further used for H&E staining, immunohistochemical analysis, and immunofluorescence staining.

For H&E staining, specimens were stained with H&E and then visualized under an Olympus BX43 light microscope (Tokyo, Japan). For immunohistochemical analysis, the slides were treated with antigen repair solution (P0081, Beyotime, Nanjing, China) for 10 min, and then with 3% hydrogen peroxide. The slides were blocked with goat serum for 30 min and treated with diluted primary antibodies in a humid chamber overnight at 4 °C. The slides were rewarmed to approximately 20 °C, incubated with secondary antibodies for 2 h, stained with 3,3′-diaminobenzidine, and counterstained with hematoxylin for nucleic staining. The slides were mounted with a neutral resin adhesive, covered with coverslips, and imaged using an Olympus BX43 light microscope (magnification, $100\times$) (Tokyo, Japan).

For immunofluorescence staining, the slides were treated with antigen repair solution and blocked with blocking buffer (5% goat serum, 2% BSA, and 0.2% Triton X-100). The diluted primary antibodies were then added to the slides and incubated overnight at 4 °C. The slides were incubated with an immunofluorescent secondary antibody for 2 h and stained with 4′,6-diamidino-2-phenylindole for 10 min (C1005, Beyotime, Nanjing, China). The slides were mounted with anti-fade fluorescence mounting medium (P0126, Beyotime, Nanjing, China) and covered with coverslips. Images were captured using a Nikon TS100 light microscope (Nikon Instruments, Tokyo, Japan) and quantified using Image-Pro Plus version 5.0 (Media Cybernetics Inc., Silver Spring, MD, USA). Information on the antibodies used is provided in Table S5.

2.8. Transmission electron microscopy

Intestinal samples were fixed in glutaraldehyde and rinsed with 0.1 M phosphate buffer thrice for 15 min. Samples were then fixed in 1% osmium tetroxide for 2 h, dehydrated serially in 30% to 100% ethyl alcohol and dehydrated further with 100% acetone twice. The samples were then treated with mixture of acetone and Epon 812 (1:1; SPI Supplies, West Chester, PA, USA) for 4 h, incubated with acetone and Epon 812 (1:2) overnight, and embedded in pure Epon 812 for 5 h. Samples were then embedded in Epon 812 at 37 °C overnight, polymerized at 60 °C for 48 h, and sliced into 80-nm sections with an ultra-microtome (EM UC7, Leica, Wetzlar, Germany) before placing on cuprum grids. Cuprum grids were stained with uranium acetate and lead citrate and dried overnight at approximately 20 °C. Images were obtained using a JEM-2100Plus transmission electron microscope (JEOL, Tokyo, Japan) at 80 kV acceleration voltage and were recorded on Kodak Electron Image Film SO-163 (Eastman Kodak Co., Rochester, NY, USA).

2.9. Statistical analysis

Statistical tests were performed using SPSS version 25 (IBM Corp., Armonk, NY, USA). Results were calculated as the mean $\pm$ SD. All results were normalized using the Shapiro−Wilk test, and Levene's test was used for homogeneity of variance before data analysis. One-way analysis of variance and Duncan's multiple range test were used to evaluate statistical differences among treatments at a level of $P < 0.05$. Correlation analyses were performed using the Pearson correlation. GraphPad version 8.0 (GraphPad Software Inc., CA, USA) was used to visualize the data.

3. Results

3.1. Intestinal histopathology and transmission electron microscopy

Following *A. hydrophila* infection, histopathological analysis (Fig. 1A) revealed that VD$_3$ deficiency was accompanied by blood capillary hyperemia and damage to the lamina propria in the PI, blood capillary hyperemia and goblet cell hyperplasia in the MI, and inflammatory cell infiltration and blood capillary hyperemia in the DI. The electron micrograph results (Fig. 1B) indicated that cell membrane was intact, and distinct junction complexes were
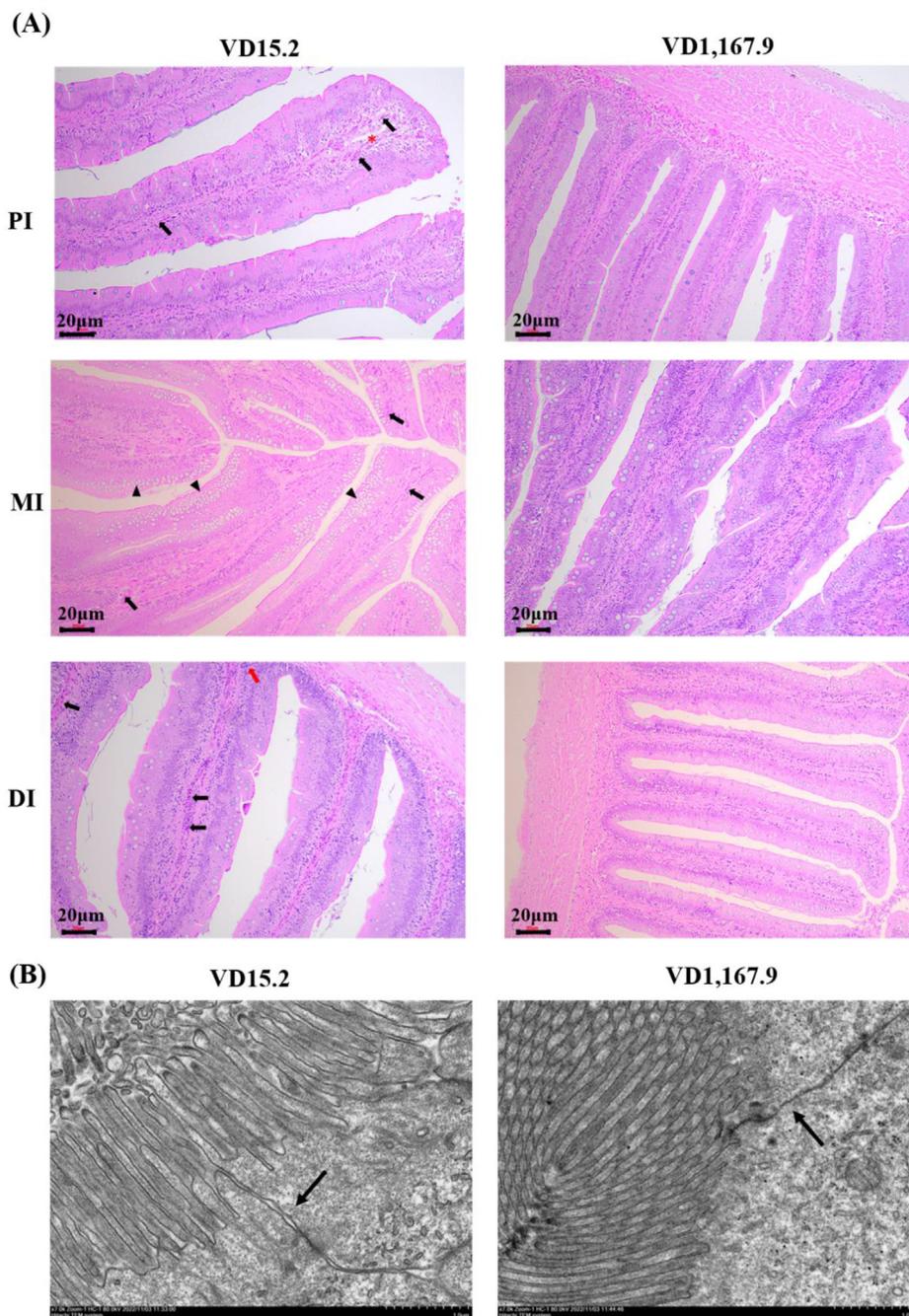

Fig. 1. Vitamin D$_3$ alleviates intestinal lesions in grass carp (*Ctenopharyngodon idella*) after *Aeromonas hydrophila* infection. (A) Hematoxylin and eosin (H&E) staining of the PI, MI, and DI (magnification, 100×). Scale bar = 20 μm. Red arrowheads, black arrowheads, and triangles show inflammatory cell infiltration, blood capillary hyperemia, and goblet cell hyperplasia, respectively; *shows damage of the lamina propria. PI = proximal intestine; MI = mid-intestine; DI = distal intestine. (B) Electron micrograph of intestinal epithelial cells showing tight junctions (magnification, 7000×). Scale bar = 1 μm. Black arrowheads show the tight junctions.
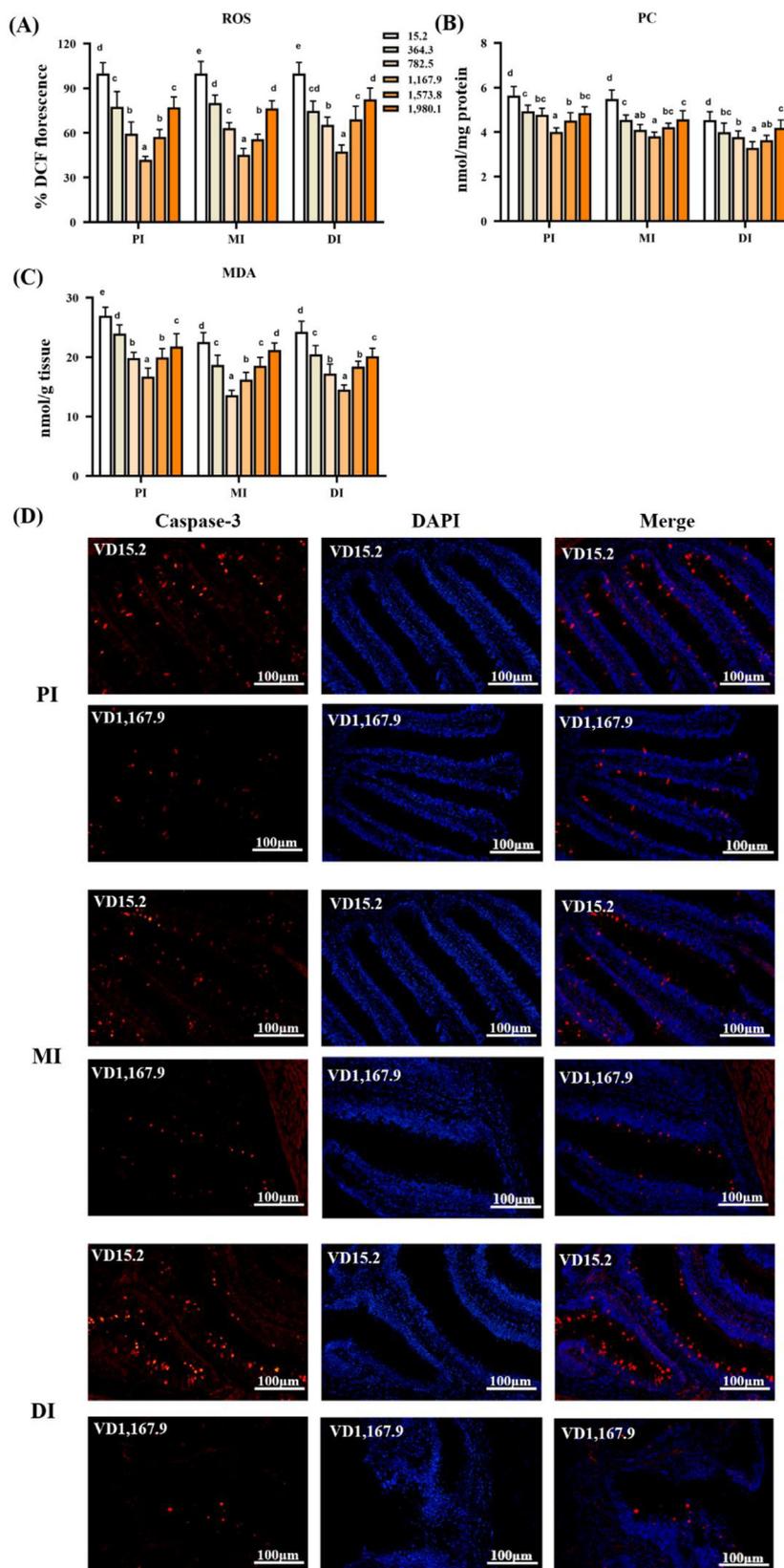
Fig. 2. Effect of dietary vitamin D$_3$ on oxidative damage and apoptosis biomarkers in the intestine of grass carp after *Aeromonas hydrophila* infection. (A−C) Oxidative damage biomarkers. ROS = reactive oxygen species (% DCF fluorescence); MDA = malondialdehyde (nmol/g tissue); PC = protein carbonyl (nmol/mg protein). (D) Immunofluorescence of caspase-3 (magnification, 200×). Scale bar = 100 μm. Caspase = cysteinyl aspartate specific proteinase. Data are shown as mean ± SD; $n = 6$ for each vitamin D$_3$ level. [a−e]Different letters above bars indicate significant differences ($P < 0.05$).

observed in the VD1,167.9 group. However, in the VD15.2 group, the structure of tight junctions became obscured and depressed. The microvilli were sparse with irregular length and arrangement in the VD15.2 group. The intestinal epithelial tight junctions were repaired with respect to structural integrity, with close intercellular connection and high electron density in the VD1,167.9 group.

3.2. Oxidative damage and apoptosis biomarkers

The effects of VD_3 on the activity of oxidative damage biomarkers and cysteinyl aspartate specific proteinase (caspase)-3 expression in the intestines are shown in Fig. 2. Reactive oxygen species (ROS), protein carbonyl (PC), and malondialdehyde (MDA) levels decreased significantly ($P < 0.05$) relative to control values with the VD1,167.9 group. Additionally, activity of all three species was lowest in the VD1,167.9 group (Fig. 2A−C). These results indicate that VD_3 protected fish intestines from oxidative injury triggered by *A. hydrophila* infection.

Excessive oxidative damage leads to apoptosis. Fig. 2D shows the immunofluorescence staining of an apoptosis biomarker (caspase-3). In the VD15.2 (unsupplemented control) group, caspase-3

was immunolocalized to select cells within the mucosal layer close to the submucosal layer in the PI and MI. Discontinuous immunostaining for caspase-3 was also observed in the PI. Continuous caspase-3 immunostaining was mainly concentrated along the mucosal and submucosal layers and the lamina propria in the DI. The positively stained sections in the VD1,167.9 group for the indices of caspase-3 were higher than those in the VD15.2 group.

3.3. Apoptosis factors

The gene expression of apoptosis factors is presented in Fig. 3. In the PI, ligands associated with apoptosis (*FasL*), c-Jun N-terminal kinase (*JNK*), BCL2-associated X (*BAX*), *p38MAPK*, and *caspase-2*, *-3*, *-8*, and *-9* were significantly downregulated in the VD782.5 group. Apoptotic protease activating factor-1 (*Apaf1*) had the lowest expression values in the VD1,167.9 group. B-cell lymphoma-2 (*Bcl-2*), inhibitor of apoptosis protein (*IAP*), and myeloid cell leukemia-1 (*Mcl-1*) reached their highest values in the VD782.5, VD782.5, and VD1,167.9 groups, respectively. In the MI, compared with the VD15.2 group, the transcription levels of *FasL*, *Apaf1*, *p38MAPK*, and *caspase-2*, *-3*, *-8*, and *-9* were decreased in the VD1,167.9 group. And *JNK* and *BAX* exhibited the lowest mRNA levels in the VD782.5 and
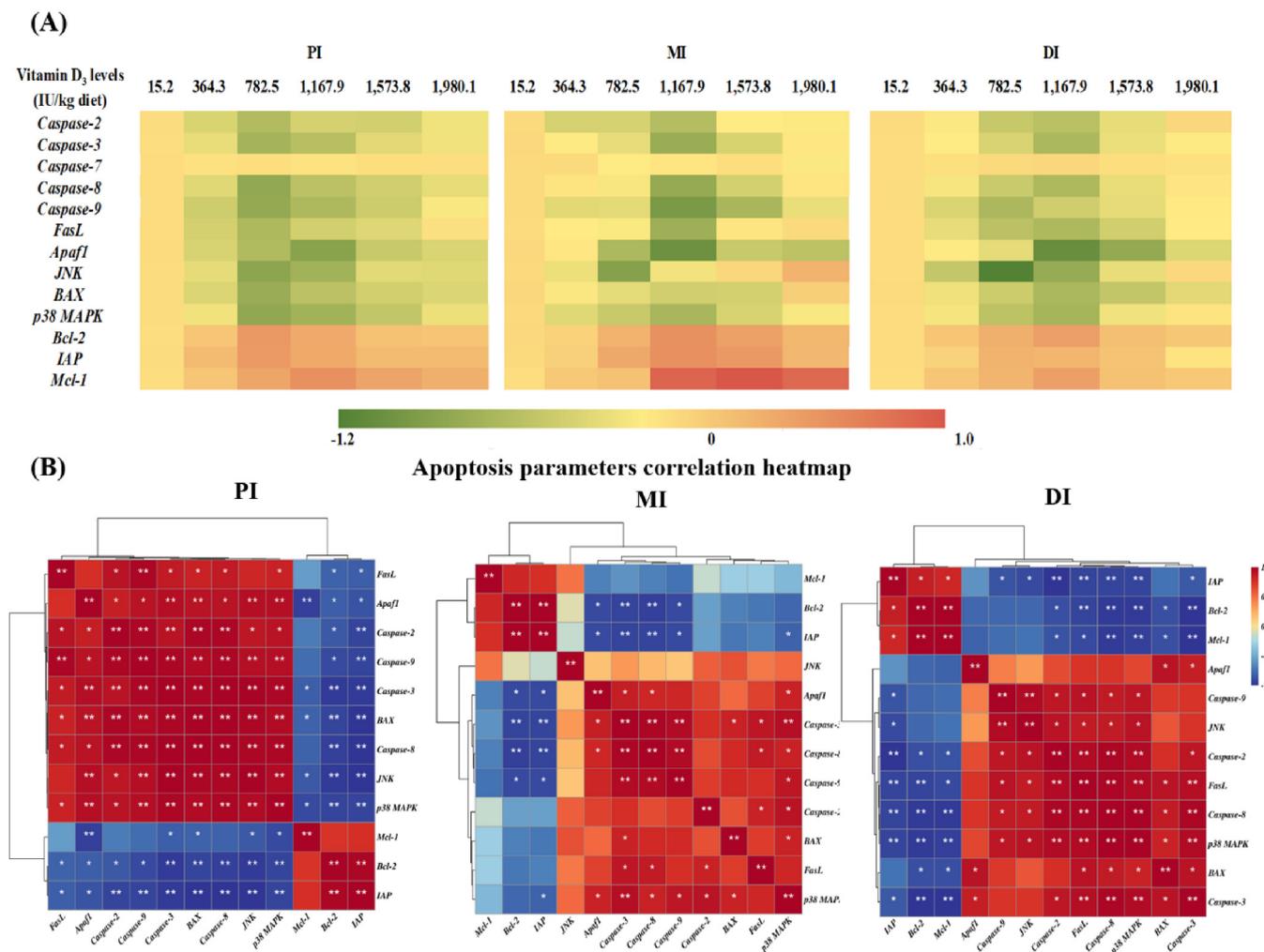

Fig. 3. Heatmaps of (A) mRNA levels and (B) correlation analysis of apoptosis-related parameters of grass carp after *Aeromonas hydrophila* infection. *Caspase* = cysteinyl aspartate specific proteinase; *FasL* = ligands associated with apoptosis; *Apaf1* = apoptotic protease activating factor-1; *JNK* = c-Jun N-terminal kinase; *BAX* = BCL2-associated X; *MAPK* = mitogen-activated protein kinase; *Bcl-2* = B-cell lymphoma-2; *IAP* = inhibitor of apoptosis protein; *Mcl-1* = myeloid cell leukemia-1; PI = proximal intestine; MI = midintestine; DI = distal intestine. The values for upregulated (red) and downregulated (green) genes represent log2 fold changes compared with values in the un-supplemented control. *Indicates $P < 0.05$, **indicated $P < 0.01$. $n = 6$ for each vitamin D_3 level.

VD1,573.8 groups, respectively. The anti-apoptotic factors *Bcl-2*, *IAP*, and *Mcl-1* were significantly upregulated with VD1,167.9, VD1,167.9, and VD1,573.8 treatments, respectively, but were downregulated at higher concentrations. In the DI, the mRNA levels of *caspase-2*, *-3*, *-8*, *FasL*, *Apaf1*, *BAX*, and *p38MAPK* downregulated with VD$_3$ administration up to the VD1,167.9 group and increased at higher concentrations. Compared with the unsupplemented control group, VD$_3$ supplementation significantly downregulated the mRNA expression of pro-inflammatory parameters (*caspase-9* and *JNK*) and upregulated the expression of the anti-inflammatory factors *Bcl-2*, *Mcl-1*, and *IAP* ($P < 0.05$). Notably, VD$_3$ did not influence *caspase-7* transcription levels in the three intestinal segments ($P > 0.05$). Pro-apoptosis gene expression was positively correlated with *p38MAPK* expression, whereas anti-apoptotic factors were negatively correlated with *p38MAPK* expression (Fig. 3B and Table S6).

We further performed protein analysis to determine the levels of apoptosis proteins (Fig. 4). In terms of apoptosis factors in the PI, levels of caspase-3, BAX, and p-p38MAPK decreased significantly ($P < 0.05$) compared with the control values in the VD1,573.8, VD1,573.8, and VD1,167.9 groups, respectively. All VD$_3$ treatments resulted in higher Bcl-2 protein levels than those in the VD15.2 group. In the MI, the protein levels of caspase-3, BAX,

and p-p38MAPK decreased significantly ($P < 0.05$) as VD$_3$ levels reached 1,167.9, 1,980.1, and 1,980.1 IU/kg, respectively. The protein levels of Bcl-2 increased as VD$_3$ reached 1,573.8 IU/kg and then decreased significantly ($P < 0.05$). In the DI, the lowest values of caspase-3, BAX, and p-p38MAPK were observed in the VD1,573.8, VD1,167.9, and VD1,980.1 groups, respectively, and the highest levels for Bcl-2 were observed in the VD1,167.9 group. No altered protein levels were observed regarding T-p38MAPK expression ($P > 0.05$).

3.4. Tight junction

The transcription levels of the tight junction genes are shown in Fig. 5A. In the PI, the VD782.5 group significantly increased the mRNA levels of *ZO-1*, claudin-c, -f, -7a, -7b, -11, -12, -15a, and -15b compared with all other treatments ($P < 0.05$). And *ZO-2*, occludin, and claudin-b reached their highest expression levels in the VD1,167.9 group. In the MI, VD1,167.9 treatment significantly elevated the gene expression of *ZO-2*, occludin, claudin-c, -7b, -11, -12, and -15a in the intestine relative to values in the VD15.2 group ($P < 0.05$), whereas VD782.5 treatment substantially increased *ZO-1* and claudin-f mRNA levels ($P < 0.05$). Claudin-b, -7a, and -15b exhibited the highest transcription levels in the VD1,980.1,
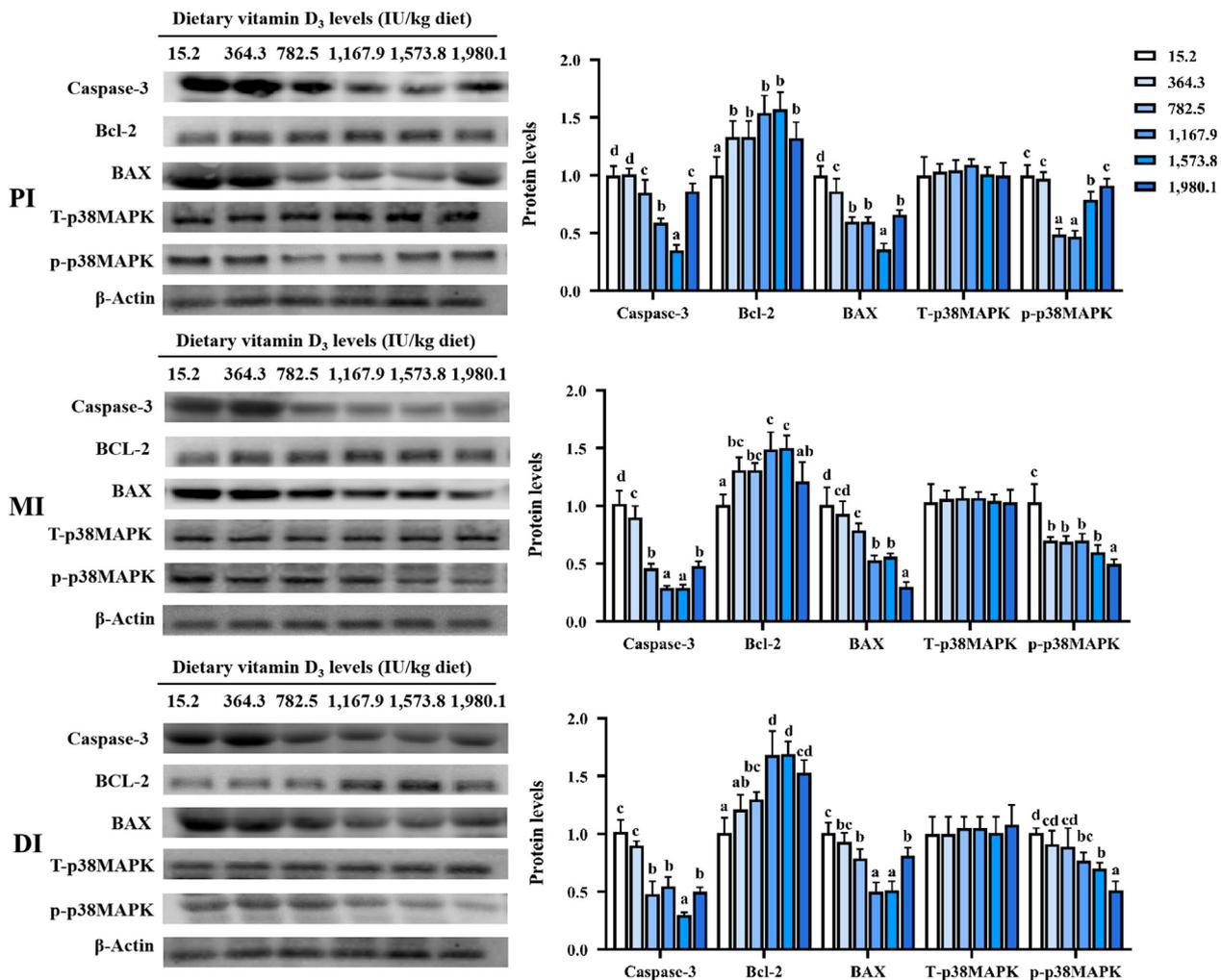

Fig. 4. Western blot analysis of apoptosis-related parameters of grass carp after *Aeromonas hydrophila* infection. Caspase = cysteinyl aspartate specific proteinase; Bcl-2 = B-cell lymphoma-2; BAX = BCL2-associated X; MAPK = mitogen-activated protein kinase; PI = proximal intestine; MI = mid-intestine; DI = distal intestine. Data are shown as mean ± SD; $n = 3$ for each vitamin D$_3$ level. $^{a–d}$Different letters above bars indicate significant differences ($P < 0.05$).

VD1,980.1, and VD1,573.8 groups, respectively. In the DI, VD782.5 markedly increased the expression of *ZO-1*, claudin-11, and -15a, and VD1,167.9 upregulated *ZO-2*, occludin, claudin-b, -c, -f, -7a, -7b, -12, and -15b ($P < 0.05$). *MLCK* reached its lowest value in the VD1,167.9 group for all three intestinal segments. Interestingly, claudin-3c mRNA levels were unaffected by dietary VD$_3$. Tight junction-related gene expression was observed to be negatively correlated with MLCK expression in three intestine segments (Fig. 5B and Table S6).

The protein levels of the tight junction genes are shown in Fig. 6. In the PI, compared with the VD15.2 group, VD1,167.9 significantly increased the protein levels of ZO-1 and occludin ($P < 0.05$). In the MI, VD$_3$ supplementation significantly enhanced ZO-1 and occludin protein levels. The highest protein levels of ZO-1 and occludin were found in the VD1,573.8 and VD1,980.1 group, respectively ($P < 0.05$). In the DI, the highest ZO-1 and occludin protein levels were found in the VD1,167.9 and VD1,573.8, respectively ($P < 0.05$). Compared with un-supplemented control group, VD$_3$ supplemented groups significantly decreased MLCK protein levels in all intestinal segments ($P < 0.05$).

Immunocytochemical and immunofluorescence staining methods were used to measure ZO-1 and occludin protein levels (Figs. 7 and 8). Immunocytochemical staining showed strong labeling in the cytoplasm of enterocytes covering the tips of villi, with a progressive decrease towards the base of the villi. Nuclear staining was also observed in the VD1,167.9 group but not in the VD15.2 group (unsupplemented control). Immunofluorescence staining showed that ZO-1 was localized in the apical region of the lateral membrane (Fig. 7).

Fig. 8 shows the location of the occludin protein in fish intestines. More intense staining of occludin in the cytoplasm of the columnar epithelium and was observed in the VD1,167.9 group than in the VD15.2 group (unsupplemented control). Immunofluorescence staining revealed that occludin localized to the apical region of the lateral membrane, consistent with distribution in the tight junctions of crypt and surface intestinal epithelial cells.

3.5. VDR expression

The transcription levels of *VDRa* were upregulated in the VD1,167.9 group ($P < 0.05$) and remained consistent at higher levels. A high mRNA level of *VDRb* was observed in the VD1,573.8 group (Fig. 9A). VD$_3$ supplementation increased VDR protein levels in the intestinal segments (Fig. 9B). VDR expression was observed to be negatively correlated with MLCK and p38MAPK expression in three intestinal segments (Fig. 9C and Table S6). Immunofluorescence for VDR (Fig. 10) showed localization to the cytoplasm and perinuclear regions, with nuclear colocalization observed as well. Samples from the VD1,167.9 group stained more positively for VDR than those from the VD15.2 group, which displayed almost no VDR expression.
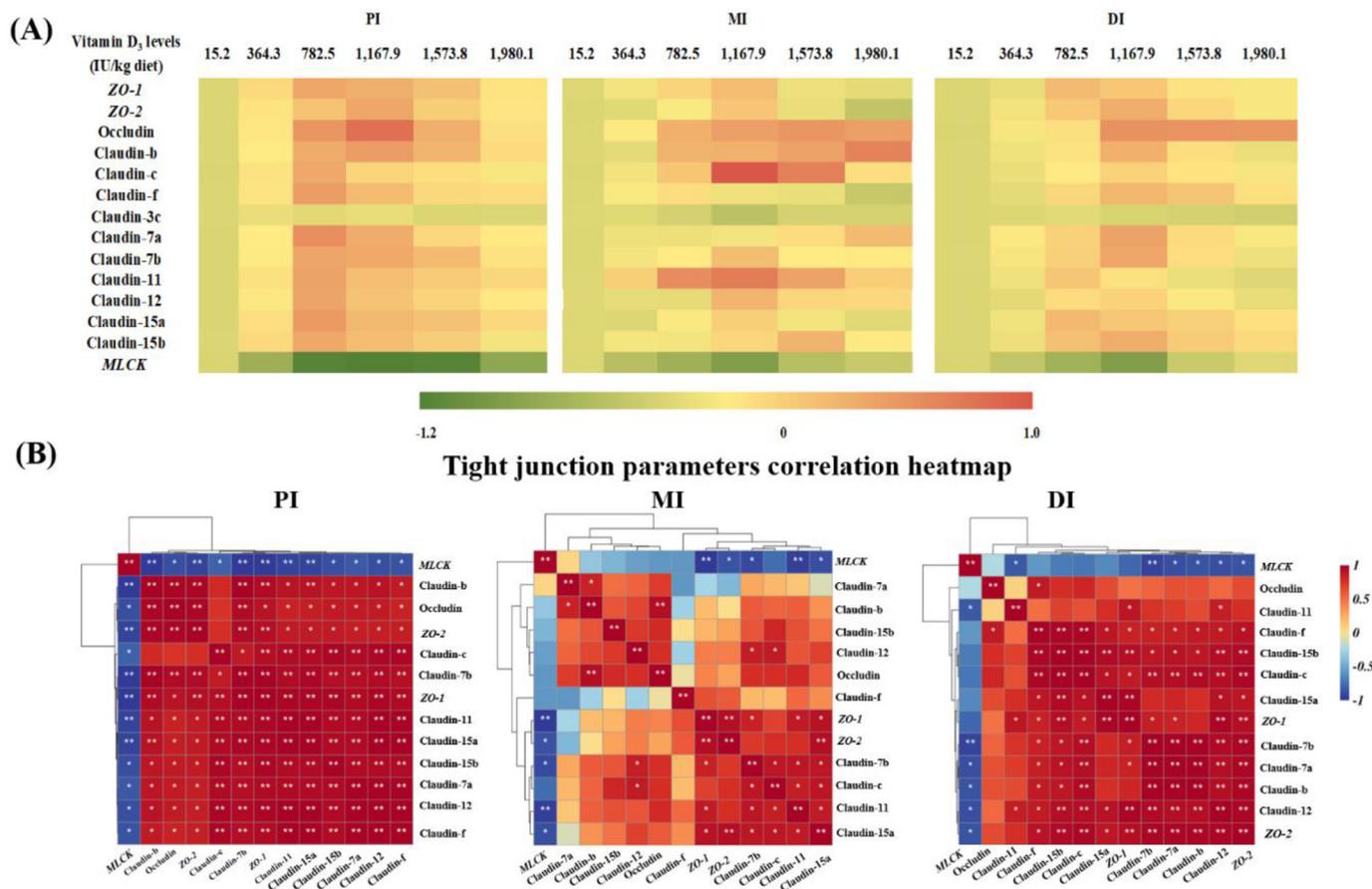

Fig. 5. Heatmaps of (A) mRNA levels and (B) correlation analysis of tight junction-related factors in grass carp intestines after *Aeromonas hydrophila* infection. ZO = zonula occludens; MLCK = myosin light chain kinase; PI = proximal intestine; MI = mid-intestine; DI = distal intestine. The values for upregulated (red) and downregulated (green) genes represent log2 fold changes compared with values in the unsupplemented control. *Indicates $P < 0.05$, **indicates $P < 0.01$. $n = 6$ for each vitamin D$_3$ level.
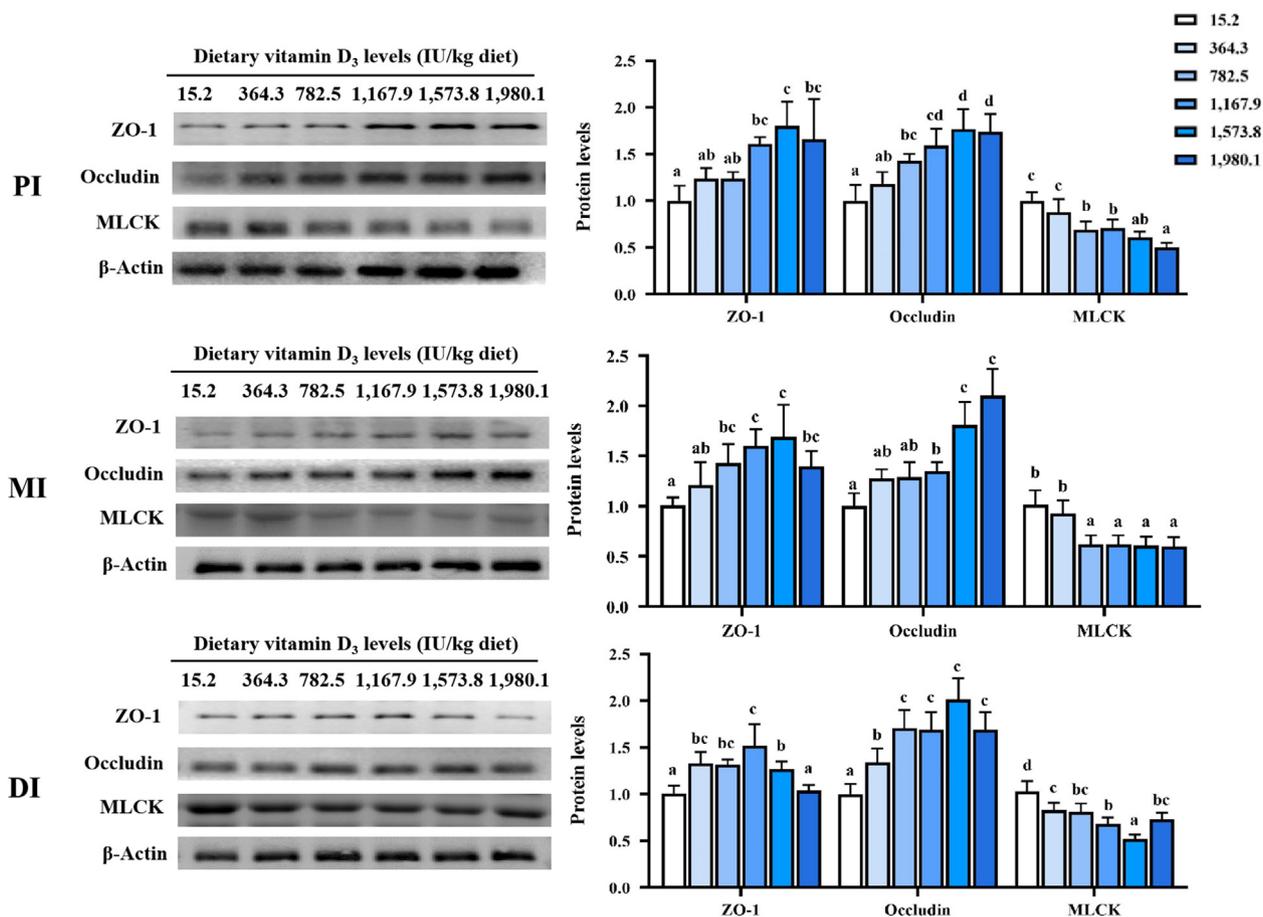
Fig. 6. Western blot analysis of tight junction-related factors in grass carp intestines after *Aeromonas hydrophila* infection. ZO = zonula occludens; MLCK = myosin light chain kinase; PI = proximal intestine; MI = mid-intestine; DI = distal intestine. Data are shown as mean ± SD; $n = 3$ for each vitamin D_3 level. [a–d]Different letters above bars indicate significant differences ($P < 0.05$).

4. Discussion

4.1. VD₃ administration enhanced disease resistance in fish intestine

Our previous study demonstrated that VD_3 improved fish growth performance, digestion, and absorptive function in different intestinal segments (Zhang et al., 2022). The distinct ultrastructure in each segment leads to diverse functions: the PI, characterized by numerous fat droplets, shows the lipid absorption status; the MI, with many pinocytotic vesicles, displays the absorption of protein macromolecules; and the DI, featuring relatively few absorptive cells and short microvilli, functions in osmoregulation (Stroband, 1977; Stroband and Debets, 1978). The structural integrity of the intestine is the structural basis for digestion and absorptive function. Herein, we investigated the intestinal structure of grass carp after pathogen infection. *A. hydrophila* is among the most frequently occurring pathogenic bacteria in grass carp and destroys the intestinal mucus layer, leaving the intestinal mucosa vulnerable to pathogens (Song et al., 2014). Pathological changes in intestinal structure are reflected in inflammatory cell infiltration, goblet cell hyperplasia (Erben et al., 2014), and blood capillary hyperemia (Wu et al., 2016). In our study, *A. hydrophila* infection resulted in grey-pink bulges and dark red granular abnormalities in the intestine. Moreover, histopathological examination revealed that dietary VD_3 deficiency caused pathological changes in fish intestines (Fig. 1), indicating damage to the integrity of the intestinal structure.

Optimal VD_3 supplementation (1,167.9 IU/kg) alleviated these histological features and decreased enteritis morbidity in a dose-dependent manner (18.34% to 6.67%). This indicates that dietary VD_3 administration protected the intestinal structure and prevented enteritis morbidity in fish, thereby enhancing resistance against *A. hydrophila* infection and maintaining organ health.

4.2. VD₃ administration strengthened intestinal integrity in grass carp

4.2.1. VD₃ administration decreased oxidative damage biomarker levels

Under pathogenic infection, organisms produce and accumulate ROS, which harms bioactive molecules such as DNA, lipids, and proteins (Tadeja et al., 2011). MDA and PC have been used to evaluate lipid peroxidation and protein oxidation, respectively (Zhang et al., 2023). In the current study, VD_3 administration reduced oxidative damage biomarker levels. These results are consistent with the findings in yellow catfish showing that VD_3 supplementation prevented lipid peroxidation and protein oxidation (Liu et al., 2021b). Dietary VD_3 decreased MDA concentration in larval Chinese mitten crab (Liu et al., 2021a). This phenomenon may be due to the structural properties of VD_3 and its metabolites. The structures of VD_3 metabolism products (25-hydroxy VD_3 and 1α,25-dihydroxy VD_3) are similar to those of cell membranes and protect cell membranes against damage from harmful bioactive molecules by stabilizing the membrane structure and diminishing
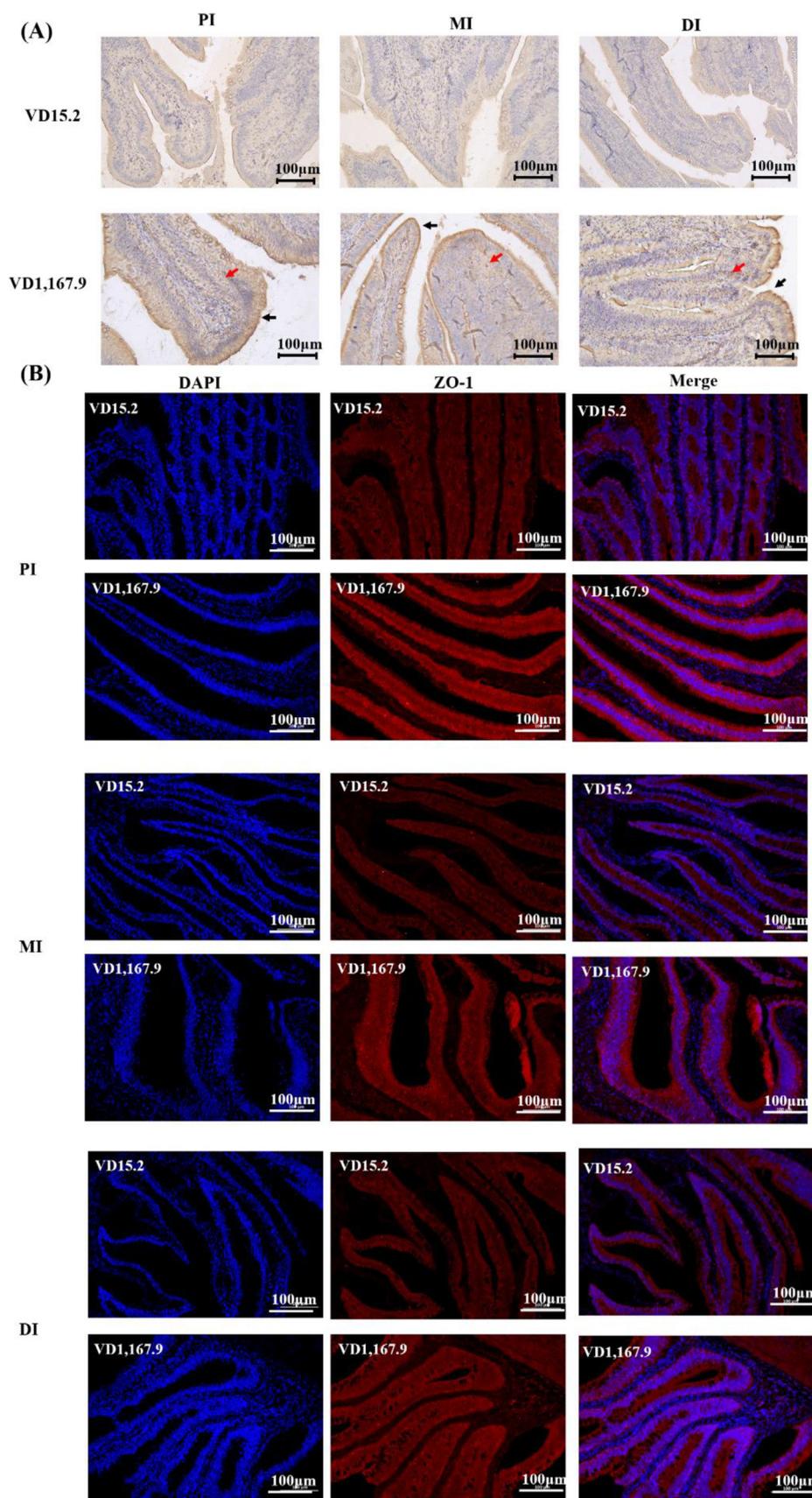
Fig. 7. Effects of vitamin D$_3$ on the expression of ZO-1 in the intestines of grass carp after *Aeromonas hydrophila* infection (magnification, 200×). (A) Immunohistochemistry results. (B) Immunofluorescence results. Scale bar = 100 μm. PI = proximal intestine; MI = mid-intestine; DI = distal intestine; ZO-1 = zonula occludens-1; n = 3 for each vitamin D$_3$ level. Black and red arrows show the location of ZO-1 protein.
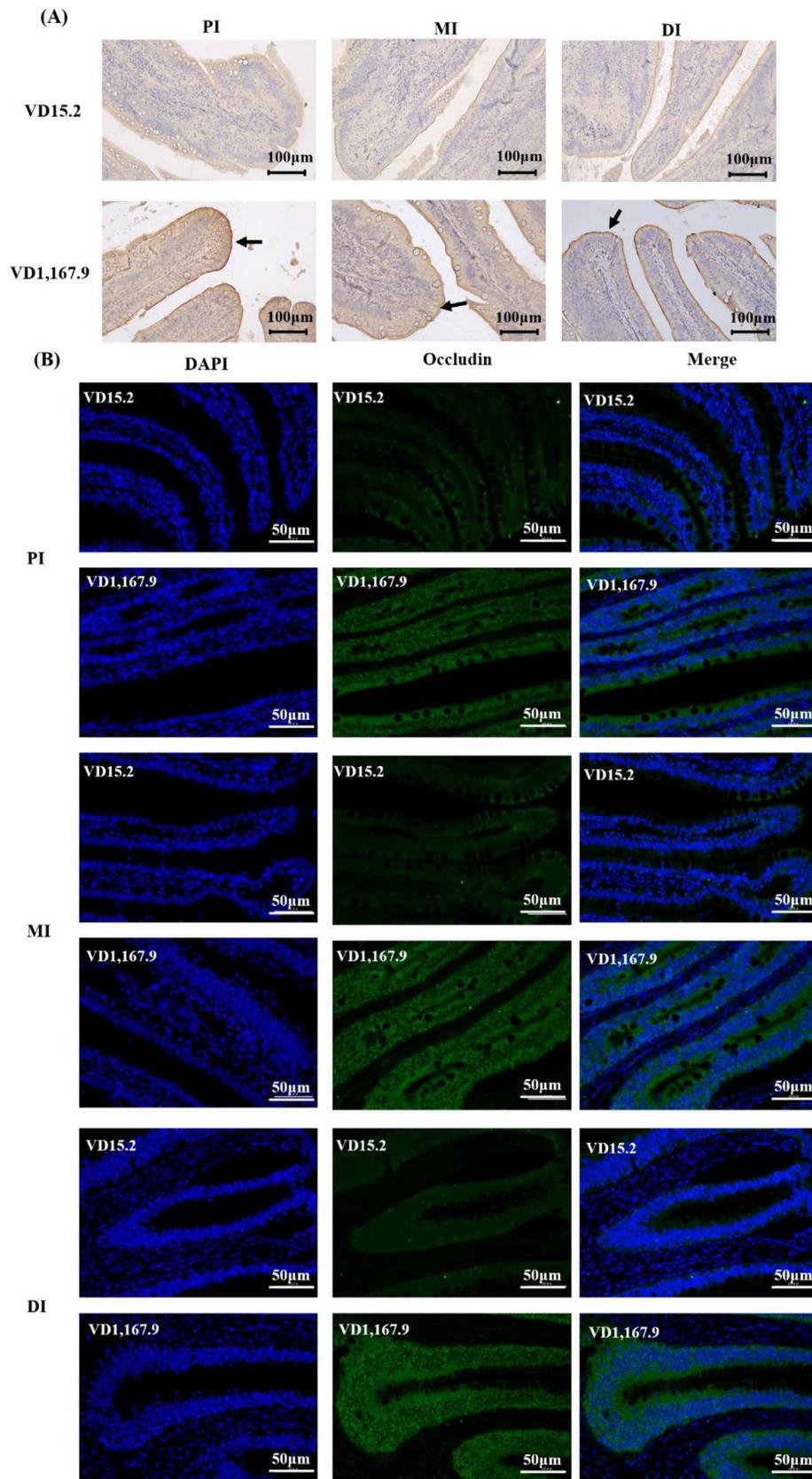
Fig. 8. Effects of vitamin D$_3$ on occludin expression in the intestines of grass carp after *Aeromonas hydrophila* infection. (A) Immunohistochemistry results (magnification, 200×). Scale bar = 100 μm. (B) Immunofluorescence results (magnification, 400×). Scale bar = 50 μm. PI = proximal intestine; MI = mid-intestine; DI = distal intestine. $n = 3$ for each vitamin D$_3$ level. Black arrows show the location of occludin protein.
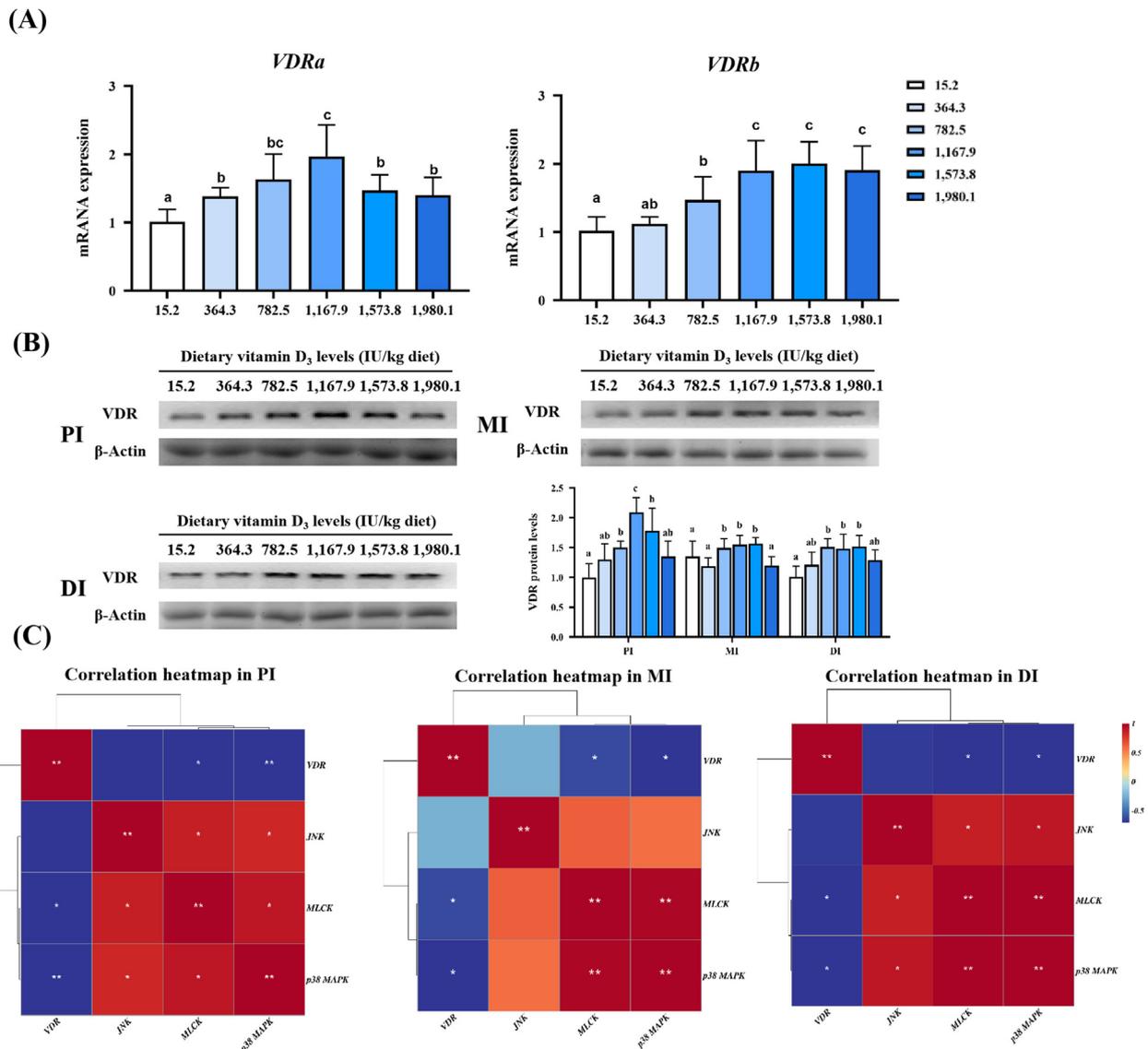
(A)

(B)

(C)

Fig. 9. Effects of vitamin D$_3$ on the (A) mRNA expression, (B) protein levels, and (C) correlation analysis of vitamin D receptor (VDR) in the intestines of grass carp after *Aeromonas hydrophila* infection. PI = proximal intestine; MI = mid-intestine; DI = distal intestine; JNK = c-Jun N-terminal kinase; MLCK = myosin light chain kinase; MAPK = mitogen-activated protein kinase. $n = 6$ for gene expression and $n = 3$ for Western blot analysis; Data are shown as mean ± SD. $^{a-c}$Different letters above bars indicate significant differences ($P < 0.05$). *Indicates $P < 0.05$, **indicated $P < 0.01$.

membrane fluidity (Tadeja et al., 2011). Moreover, the gene coding for superoxide dismutase, which is responsible for scavenging free radicals, is the target of VDR (Zhong et al., 2014). VDR mediates the enhancement of antioxidant capacity by increasing antioxidant enzyme expression (Zhang et al., 2023). Compared with those under optimal VD$_3$ supplementation (VD1,167.9 group), MDA and PC levels were elevated under excess VD$_3$, potentially because excess VD$_3$ is stored and causes lipotoxicity in vivo (Wang et al., 2015a).

4.2.2. VD$_3$ administration alleviated cell apoptosis caused by pathogen infection

Excessive accumulation of oxidative damage biomarkers is associated with cell apoptosis. We next investigated the influence of VD$_3$ on cell apoptosis in the three intestinal segments. Caspase-3 is essential for apoptosis-related processes and is indispensable for apoptotic chromatin coagulation and DNA fragmentation (Porter and Jänicke, 1999). Our results demonstrated that caspase-3 was localized in the mucosa, submucosa, and lamina propria. The VD15.2

group showed a higher positive fluorescence intensity in the DI, indicating that more cell apoptosis occurred in the DI than in the PI and MI. These differences may be related to endocrine cells. The DI segment possesses fewer endocrine cells than the PI and MI segments in grass carp (Ni and Wang, 1999). The endocrine system has been demonstrated to modulate immunity and thus plays a crucial role in responses to pathogen challenges in chickens (Kaiser et al., 2009). Therefore, we inferred that the weak interaction of endocrine immunity leads to apoptosis in the DI. Additionally, *caspase-3* expression was lowest in all intestinal segments in the VD1,167.9 group, indicating that VD$_3$ inhibited cell apoptosis. Similar results found that VD$_3$ supplementation decreased gene expression of *caspase-3* in yellow catfish intestines (Liu et al., 2021b).

Two major advances in understanding the molecular mechanisms of the death receptor and mitochondrial apoptosis pathways have been reported (Gupta, 2002). The death receptor pathway (*FasL/caspase-8/[caspase-3* and *caspase-7]*) and mitochondrial pathway ([*BAX, Bcl-2,* and *Mcl-1]/Apaf-1/caspase-9/[caspase-3* and
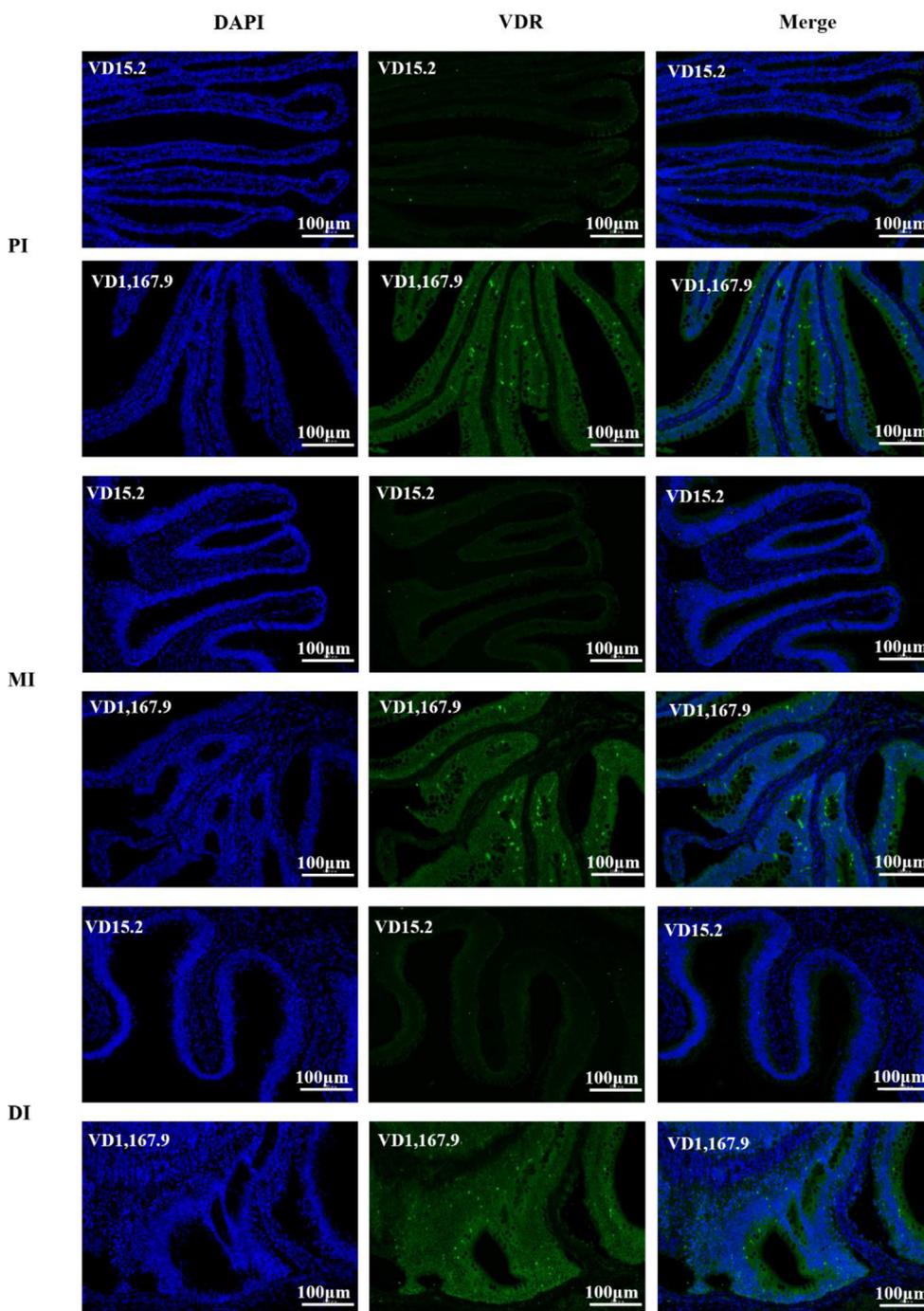
Fig. 10. Effects of vitamin D_3 on the expression of vitamin D receptor (VDR) in the intestines of grass carp after *Aeromonas hydrophila* infection (magnification, 200×). Scale bar = 100 μm. PI = proximal intestine; MI = mid-intestine; DI = distal intestine. $n = 3$ for each vitamin D_3 level in immunofluorescence analysis.

caspase-7]) are mediated by p38MAPK and JNK signaling, respectively (Cai et al., 2019; Chen et al., 2010; Tanel and Averill-Bates, 2007). The present study showed that dietary VD_3 decreased the transcription levels of *FasL*, *Apaf-1*, *JNK*, *BAX*, *p38MAPK*, and *caspase-2*, *-3*, *-8*, *-9* and upregulated *Bal-2*, *IAP*, and *Mcl-2* in the three intestinal segments. Similar results in vitro and in vivo were observed in a previous study, which reported that VD_3 supplementation decreased *caspase-3* and *BAX* mRNA levels and up-regulated *Bcl-2* expression under lipopolysaccharide-induced injury to primary intestinal epithelial cells in trout (Shao et al., 2022). Moreover, correlation analysis confirmed that pro-apoptosis gene expression

was positively correlated with *p38MAPK* and *JNK* mRNA levels, whereas anti-apoptotic factors were negatively correlated. These results indicated that VD_3 suppresses excessive apoptosis during pathogen infection, partially in association with the p38MAPK and JNK pathways.

4.2.3. VD_3 administration alleviated the damage of tight junctions

ZO-1 and occludin, the vital components of tight junctions, are critical for maintaining connections between intestinal epithelial cells (Wang et al., 2015a). Immunocytochemical and immunofluorescence staining showed that ZO-1 was labeled in the nuclei and

outer tips of columnar epithelial cells in the fish intestines. In pigs, ZO-1 staining was observed in the epithelial cell boundary and apical cell membrane (Ko et al., 2014), and ZO-1 was found in the margin of the intestinal epithelium in mouse intestines (Ahmad et al., 2008). Unlike in mammals, ZO-1 staining has also been detected in the nuclei of fish cells. In cultured epithelial cells, ZO-1 accumulates in the nucleus at wounding sites, presenting evidence that ZO-1 can be detected in the nucleus under cell growth conditions (Gottardi et al., 1996). Moreover, in this study, the staining of ZO-1 was highly positive in the VD1,167.9 group, which suggests that during pathogen infection, VD3 supplementation promotes cell regeneration and repair. Immunocytochemical and immunofluorescence staining showed that occludin was located in the lateral membrane of columnar epithelia. In the rat ileum, occludin protein was irregularly distributed at the outer enterocyte periphery (Mazzon et al., 2002), consistent with our results. We observed increased occludin protein expression in response to VD1,167.9 supplementation when compared with that in the control group.

Tight junctions form a regulated barrier in the paracellular pathway between epithelial and endothelial cells and contain integral membrane proteins (Luo et al., 2014), which are associated with *MLCK* (Wen et al., 2014). VD3 supplementation (1,167.9 IU/kg) upregulated *ZO-1* and *-2*, occludin, and claudin-b, -c, -f, -7a, -7b, -11, -12, -15a, and -15b mRNA levels and decreased MLCK transcriptional levels compared with VD15.2 group. In a previous study, VD3 supplementation enhanced mRNA levels of *ZO-1* under lipopolysaccharide-induced injury in trout intestines (Shao et al., 2022). Moreover, yellow catfish fed with VD3 exhibited enhanced expression levels of tight junction protein genes, including claudin-1, claudin-2, claudin-5, *MLCK*, claudin-12, occludin and *ZO-1* under lipopolysaccharide-induced intestinal injury (Liu et al., 2021b). Correlation analysis showed that tight junction-related gene expression was negatively correlated with *MLCK*, suggesting that VD3 positively affected tight junction function via *MLCK* inhibition in fish intestines.

4.3. VD3 administration increased VDR expression

VDR mediates the biological action of VD3. Immunofluorescence staining revealed that VDR was localized in the cytoplasm, perinuclear region, and nucleus. VDR belongs to the steroid receptor family and is evolutionarily conserved among fish, birds, and mammals (Haussler et al., 2013). Our study demonstrated that dietary VD3 upregulated both *VDRa* and *VDRb* transcription levels. Correlation analysis showed that VDR expression was observed to be negatively correlated with MLCK and p38MAPK expression in the three intestinal segments. A previous study demonstrated that VDR plays a crucial role in apoptosis and tight junctions. In rats, VDR inhibited the apoptotic cascade in hippocampal CA1 neurons of global cerebral ischemia (Guo et al., 2019) and reduced high glucose-induced apoptosis by inhibiting oxidative stress in endothelial cells (Zhang et al., 2018). VDR deletion led to damaged tight junctions in mouse lung (Chen et al., 2018). Both *VDRa* and *VDRb* were expressed during the development (11, 22, and 45 d after hatching) of sea bass larvae fed different VD3 diets (Darias et al., 2010). *VDRa* and *VDRb* were both expressed in trout intestinal cells under lipopolysaccharide-induced injury (Shao et al., 2022). Few studies have focused on the different functions of VDRa and VDRb in fish. Lin et al. (2012) showed that *VDRa*, but not *VDRb*, regulates epithelial calcium channels to increase calcium uptake. In zebrafish, VDRb, but not VDRa, deletion results in abnormalities in the craniofacial cartilage (Kwon, 2019). VDRs genes are universally expressed in fish, and different tissues exhibit different distribution patterns. In the Atlantic salmon, both VDRs show high expression in intestinal segments (Lock et al., 2007). Our unpublished data from

grass carp research also show that VDR transcription levels in intestines are higher than those in other tissue. These observations support our conclusion that both VDRs play a significant role in maintaining intestinal function, and their specific functions should be explored further.

5. Conclusions

In the current study, we systematically examined the effect of VD3 on apoptosis and tight junctions. To the best of our knowledge, this study is the first to explore the effects of dietary VD3 on tight junctions and signaling pathways associated with VDR isoforms in fish intestines. Under *A. hydrophila* challenge, VD3 supplementation prevented intestinal damage, decreased the expression of oxidative damage markers (ROS, MDA, and PC), inhibited excessive apoptosis by decreasing p38MAPK and JNK expression, and improved tight junction protein expression by restraining MLCK signaling. VD3 plays a significant role in preventing apoptosis and regulating tight junctions in grass carp intestines under pathogen infection. According to the results of quadratic regression analysis of ROS in the PI (Fig. S1), the dietary VD3 requirement of growing grass carp was estimated to be 1,180.00 IU/kg. Our work provides a new perspective on disease-resistant nutritional intervention in aquaculture and offers insight regarding the molecular mechanisms by which vitamins support the intestinal structural integrity of fish.

Author contributions

Yao Zhang: Investigation, Manuscript writing, Formal analysis. **Xiao-Qiu Zhou, Wei-Dan Jiang:** Data curation. **Pei Wu**, **Yang Liu:** Methodology. **Hong-Mei Ren:** Management. **Lu Zhang, Hai-Feng Mi, Ling Tang, Cheng-Bo Zhong:** Resources. **Lin Feng:** Conceptualization, Supervision. **Lin Feng** had primary responsibility for the final content of the manuscript. All authors carefully read and approved the final revision of the manuscript.

Declaration of competing interest

We declare that we have no financial and personal relationships with other people or organizations that can inappropriately influence our work, and there is no professional or other personal interest of any nature or kind in any product, service and/or company that could be construed as influencing the content of this paper.

Acknowledgments

Appendix supplementary data

Supplementary data to this article can be found online at https://doi.org/10.1016/j.aninu.2023.07.010.

References

Abreu RE, Magalhães TC, Souza RC, Oliveira ST, Ibelli AM, Demarqui FN, et al. Environmental factors on virulence of *Aeromonas hydrophila*. Aquac Int 2018;26(2):495—507. https://doi.org/10.1007/s10499-017-0230-2.

Ahmad R, Tripathi AK, Tripathi P, Singh S, Singh R, Singh RK. Malondialdehyde and protein carbonyl as biomarkers for oxidative stress and disease progression in

patients with chronic myeloid leukemia. In Vivo 2008;22(4):525–8. https://doi.org/10.1089/hum.2007.130.

AOAC. Official Methods of Analysis. 18th ed. Gaithersburg, MD: AOAC International; 2005.

Berkes J, Viswanathan VK, Savkovic SD, Hecht G. Intestinal epithelial responses to enteric pathogens: effects on the tight junction barrier, ion transport, and inflammation. Gut 2003;52(3):439–51. https://doi.org/10.1136/gut.52.3.439.

Cai G, Si M, Li X, Zou H, Gu J, Yuan Y, Liu X, Liu Z, Bian J. Zearalenone induces apoptosis of rat Sertoli cells through Fas-Fas ligand and mitochondrial pathway. Environ Toxicol 2019;34(4):424–33. https://doi.org/10.1002/tox.22696.

Chen YJ, Liu WH, Kao PH, Wang JJ, Chang LS. Involvement of p38 MAPK- and JNK-modulated expression of Bcl-2 and Bax in Naja nigricollis CMS-9-induced apoptosis of human leukemia K562 cells. Toxicon 2010;55(7):1306–16. https://doi.org/10.1016/j.toxicon.2010.01.024.

Chen H, Lu R, Zhang YG, Sun J. Vitamin D receptor deletion leads to the destruction of tight and adherens junctions in lungs. Tissue Barriers 2018;6(4):1–13. https://doi.org/10.1080/21688370.2018.1540904.

Chin AC, Flynn AN, Fedwick JP, Buret AG. The role of caspase-3 in lipopolysaccharide-mediated disruption of intestinal epithelial tight junctions. Can J Physiol Pharmacol 2006;84:1043–50. https://doi.org/10.1139/y06-056.

Christakos S, Dhawan P, Verstuyf A, Verlinden L, Carmeliet G. Vitamin D: metabolism, molecular mechanism of action, and pleiotropic effects. Physiol Rev 2016;96(1):365–408. https://doi.org/10.1152/physrev.00014.2015.

Craig TA, Sommer S, Sussman CR, Grande JP, Kumar R. Expression and regulation of the vitamin D receptor in the zebrafish, *Danio rerio*. J Bone Miner Res 2008;23(9):1486–96. https://doi.org/10.1359/jbmr.080403.

Darias MJ, Mazurais D, Koumoundouros G, Glynatsi N, Christodoulopoulou S, Huelvan C, et al. Dietary vitamin D₃ affects digestive system ontogenesis and ossification in European sea bass (*Dicentrachus labrax*, Linnaeus, 1758). Aquaculture 2010;298:300–7. https://doi.org/10.1016/j.aquaculture.2009.11.002.

Elizondo RA, Yin ZH, Lu XW, Watsky MA. Effect of vitamin D receptor knockout on cornea epithelium wound healing and tight junctions. Cornea 2014;55(8):5245–51. https://doi.org/10.1167/iovs.13-13553.

Erben U, Loddenkemper C, Doerfel K, Spieckermann S, Haller D, Heimesaat MM, et al. A guide to histomorphological evaluation of intestinal inflammation in mouse models. Int J Clin Exp Pathol 2014;7(8):4557–76.

FAO. The State of World Fisheries and Aquaculture 2020: sustainability in action. Rome, Italy: Food and Agriculture Organisation of the United Nations; 2020. p. 9–65.

Feng Y, Bi PP, Wang C, Li J, Liu XQ, Kuang SH. Conditional loss of Pten in myogenic progenitors leads to postnatal skeletal muscle hypertrophy but age-dependent exhaustion of satellite cells. Cell Rep 2016;17(9):2340–53. https://doi.org/10.1016/j.celrep.2016.11.002.

Gottardi CJ, Arpin M, Fanning AS, Louvard D. The junction-associated protein, zonula occludens-1, localizes to the nucleus before the maturation and during the remodeling of cell-cell contacts. Proc Natl Acad Sci U S A 1996;93(20):10779–84.

Granada L, Sousa N, Lopes S, Lemos MF. Is integrated multitrophic aquaculture the solution to the sectors' major challenges?–a review. Rev Aquac 2016;8(3):283–300. https://doi.org/10.1111/raq.12093.

Guo X, Yuan J, Wang J, Cui C, Jiang P. Calcitriol alleviates global cerebral ischemia-induced cognitive impairment by reducing apoptosis regulated by VDR/ERK signaling pathway in rat hippocampus. Brain Res 2019;1724(1):146430. https://doi.org/10.1016/j.brainres.2019.146430.

Gupta S. Molecular signaling in death receptor and mitochondrial pathways of apoptosis (Review). Int J Oncol 2002;22(1):15–20. https://doi.org/10.3892/ijo.22.1.15.

Haussler MR, Whitfield GK, Kaneko I, Haussler CA, Hsieh D, Hsieh JC, et al. Molecular mechanisms of vitamin D action. Calcif Tissue Int 2013;92(2):77–98. https://doi.org/10.1007/s00223-012-9619-0.

Kaiser P, Wu Z, Rothwell L, Fife M, Gibson M, Poh TY, Shini A, Bryden W, Shini S. Prospects for understanding immune–endocrine interactions in the chicken. Gen Comp Endocrinol 2009;163(1–2):83–91. https://doi.org/10.1016/j.ygcen.2008.09.013.

Ko JY, Kim EA, Lee JH, Kang MC, Lee JS, Kim JS, et al. Protective effect of aquacultured flounder fish-derived peptide against oxidative stress in zebrafish. Fish Shellfish Immunol 2014;36(1):320–3. https://doi.org/10.1016/j.fsi.2013.11.018.

Kong WG, Li SS, Chen XX, Huang YQ, Tang Y, Wu ZX, et al. A study of the damage of the intestinal mucosa barrier structure and function of *Ctenopharyngodon idella* with *Aeromonas hydrophila*. Fish Physiol Biochem 2017;43:1223–35. https://doi.org/10.1007/s10695-017-0366-z.

Kwon HJ. Vitamin D receptor signaling regulates craniofacial cartilage development in zebrafish. J Dev Biol 2019;7(2):13. https://doi.org/10.3390/jdb7020013.

Li D, Li C, Zhang G, Peng X, Zhou D, Li X. Effects of vitamin D₃ supplemental level on cell proliferation and apoptosis of peripheral immune related tissues in *Monopterus albus*. Chin J Anim Nutr 2013;25(4):752–60. https://doi.org/10.3390/ani13040711.

Li XX, Chen FY, Huang D, Guo YL, Wu YJ, Wu CL, et al. Interactions of dietary carbohydrate and vitamin D3 on growth performance, insulin signaling pathway and glucose metabolism in juvenile abalone *Haliotis discus hannai*. Aquaculture 2021;542(15):736908. https://doi.org/10.1016/j.aquaculture.2021.736908.

Lin CH, Su CH, Tseng DY, Ding FC, Hwang PP. Action of vitamin D and the receptor, VDRa, in calcium handling in zebrafish (*Danio rerio*). PLoS One 2012;7(9):e45650. https://doi.org/10.1371/journal.pone.0045650.

Liu S, Wang X, Bu X, Lin Z, Li E, Shi Q, et al. Impact of dietary vitamin D₃ supplementation on growth, molting, antioxidant capability, and immunity of juvenile Chinese mitten crabs (*Eriocheir sinensis*) by metabolites and vitamin D receptor. J Agric Food Chem 2021a;69(43):12794–806. https://doi.org/10.1021/acs.jafc.1c04204.

Liu Y, Meng F, Wang S, Xia S, Wang R. Vitamin D3 mitigates lipopolysaccharide-induced oxidative stress, tight junction damage and intestinal inflammatory response in yellow catfish, *Pelteobagrus fulvidraco*. Comp Biochem Physiol C Toxicol Pharmacol 2021b;243:108982. https://doi.org/10.1016/j.cbpc.2021.108982.

Lock EJ, Ørnsrud R, Aksnes L, Spanings FAT, Waagbø R, Flik G, et al. The vitamin D receptor and its ligand 1α, 25-dihydroxyvitamin D3 in Atlantic salmon (*Salmo salar*). J Endocrinol 2007;193(3):459–71. https://doi.org/10.1677/JOE-06-0198.

Lu R, Zhang YG, Xia Y, Sun J. Imbalance of autophagy and apoptosis in intestinal epithelium lacking the vitamin D receptor. FASEB J 2019;33:11845–56. https://doi.org/10.1096/fj.201900727R.

Luo JB, Feng L, Jiang WD, Liu Y, Wu P, Jiang J, et al. The impaired intestinal mucosal immune system by valine deficiency for young grass carp (*Ctenopharyngodon idella*) is associated with decreasing immune status and regulating tight junction proteins transcript abundance in the intestine. Fish Shellfish Immunol 2014;40(1):197–207. https://doi.org/10.1016/j.fsi.2014.07.003.

Mazzon E, Sturniolo GC, Puzzolo D, Frisina N, Fries W. Effect of stress on the paracellular barrier in the rat ileum. Gut 2002;51:507. https://doi.org/10.1073/pnas.93.20.10779.

Ni DS, Wang JG. Biology and diseases of grass carp. 1st ed. Beijing: Science Press; 1999. p. 29–33 [in Chinese].

Niessen CM. Tight junctions/adherens junctions: basic structure and function. J Invest Dermatol 2007;127(11):2525–32. https://doi.org/10.1038/sj.jid.5700865.

Nong KY, Liu YM, Fang X, Qin XY, Liu ZN, Zhang HW. Effects of the vitamin D3 on alleviating the oxidative stress induced by diquat in Wenchang chickens. Animals 2023;13(4):711. https://doi.org/10.3390/ani13040711.

Porter AG, Jänicke RU. Emerging roles of caspase-3 in apoptosis. Cell Death Differ 1999;6(2):99–104. https://doi.org/10.1038/sj.cdd.4400476.

Salinas I, Parra D. 6 - Fish mucosal immunity: intestine. In: Beck BH, Peatman E, editors. Mucosal health in aquaculture. San Diego: Academic Press; 2015. p. 135–70.

Schroers V, van der Marel M, Neuhaus M, Steinhagen D. Changes of intestinal mucus glycoproteins after peroral application of *Aeromonas hydrophila* to common carp (*Cyprinus carpio*). Aquaculture 2009;288(3–4):184–9. https://doi.org/10.1016/j.aquaculture.2008.12.013.

Shah S, Chen J, Han Q, Xu Y, Teng X. Ammonia inhalation impaired immune function and mitochondrial integrity in the broilers bursa of fabricius: implication of oxidative stress and apoptosis. Ecotoxicol Environ Saf 2019;190(1):110078. https://doi.org/10.1016/j.ecoenv.2019.110078.

Shao R, Liu JY, Lan YW, Liao XM, Zhang JJ, Xu WQ, et al. Vitamin D impacts on the intestinal health, immune status and metabolism in turbot (*Scophthalmus maximus* L.). Br J Nutr 2022;128(11):1–14. https://doi.org/10.1017/S0007114522000125.

Song XH, Zhao J, Bo YX, Liu ZJ, Wu K, Gong CL. *Aeromonas hydrophila* induces intestinal inflammation in grass carp (*Ctenopharyngodon idella*): an experimental model. Aquaculture 2014;434(20):171–8. https://doi.org/10.1016/j.aquaculture.2014.08.015.

Stroband H. Growth and diet dependant structural adaptations of the digestive tract in juvenile grass carp (*Ctenopharyngodon idella*). J Fish Biol 1977;11(2):167–74. https://doi.org/10.1016/j.aquaculture.2020.736086.

Stroband HW, Debets FM. The ultrastructure and renewal of the intestinal epithelium of the juvenile grass carp, *Ctenopharyngodon idella*. Cell Tissue Res 1978;187(2):181–200. https://doi.org/10.1007/BF00224364.

Tadeja R, Damjana R, Jean-Marc P, Katalin M. Interplay between cholesterol and drug metabolism. Biochim Biophys Acta Proteins Proteom 2011;1814:146–60. https://doi.org/10.1016/j.bbapap.2010.05.014.

Tanel A, Averill-Bates DA. Activation of the death receptor pathway of apoptosis by the aldehyde acrolein. Free Radic Biol Med 2007;42(6):798–810. https://doi.org/10.1016/j.freeradbiomed.2006.12.009.

Tian L, Zhou XQ, Jiang WD, Liu Y, Wu P, Jiang J, et al. Sodium butyrate improved intestinal immune function associated with NF-kappa B and p38MAPK signalling pathways in young grass carp (*Ctenopharyngodon idella*). Fish Shellfish Immunol 2017;66:548–63. https://doi.org/10.1016/j.fsi.2017.05.049.

Wang B, Feng L, Jiang WD, Wu P, Kuang SY, Jiang J, et al. Copper-induced tight junction mRNA expression changes, apoptosis and antioxidant responses via NF-kappa B, TOR and Nrf2 signaling molecules in the gills of fish: preventive role of arginine. Aquat Toxicol 2015a;158:125–37. https://doi.org/10.1016/j.aquatox.2014.10.025.

Wang PF, Yao DH, Hu YY, Li Y. Vitamin D improves intestinal barrier function in cirrhosis rats by upregulating heme oxygenase-1 expression. Biomol Ther 2019;27(2):222. https://doi.org/10.4062/biomolther.2018.052.

Wang YP, Lu Y, Zhang Y, Ning ZM, Li Y, Zhao Q, et al. The draft genome of the grass carp (*Ctenopharyngodon idellus*) provides insights into its evolution and vegetarian adaptation. Nat Genet 2015b;47(6):962. https://doi.org/10.1038/ng.3280.

Wen HL, Feng L, Jiang WD, Liu Y, Jiang J, Li SH, et al. Dietary tryptophan modulates intestinal immune response, barrier function, antioxidant status and gene expression of TOR and Nrf2 in young grass carp (*Ctenopharyngodon idella*). Fish Shellfish Immunol 2014;4(1):275–87. https://doi.org/10.1016/j.fsi.2014.07.004.

Wu P, Jiang WD, Jiang J, Zhao J, Liu Y, Zhang YA, et al. Dietary choline deficiency and excess induced intestinal inflammation and alteration of intestinal tight junction protein transcription potentially by modulating NF-κB, STAT and p38 MAPK

signaling molecules in juvenile Jian carp. Fish Shellfish Immunol 2016;58: 462–73. https://doi.org/10.1016/j.fsi.2016.09.055.

Wu C, Lu B, Wang Y, Jin C, Zhang Y, Ye J. Effects of dietary vitamin D₃ on growth performance, antioxidant capacities and innate immune responses in juvenile black carp *Mylopharyngodon piceus*. Fish Physiol Biochem 2020;46(6):2243–56. https://doi.org/10.1007/s10695-020-00876-8.

Xu HJ, Jiang WD, Feng L, Liu Y, Wu P, Jiang J, et al. Dietary vitamin C deficiency depresses the growth, head kidney and spleen immunity and structural integrity by regulating NF-kappa B, TOR, Nrf2, apoptosis and MLCK signaling in young grass carp (*Ctenopharyngodon idella*). Fish Shellfish Immunol 2016;52: 111–38. https://doi.org/10.1016/j.fsi.2016.02.033.

Yuan ZH, Feng L, Jiang WD, Wu P, Liu Y, Kuang SY, et al. Dietary choline deficiency aggravated the intestinal apoptosis in association with the MAPK signalling pathways of juvenile grass carp (*Ctenopharyngodon idella*). Aquaculture 2021;532(15):736046. https://doi.org/10.1016/j.aquaculture.2020.736046.

Zhang YG, Wu S, Sun J. Vitamin D, vitamin D receptor and tissue barriers. Tissue Barriers 2013;1(1):e23118. https://doi.org/10.4161/tisb.23118.

Zhang M, Lin L, Xu C, Chai D, Peng F, Lin J. VDR agonist prevents diabetic endothelial dysfunction through inhibition of prolyl isomerase-1-mediated mitochondrial oxidative stress and inflammation. Oxid Med Cell Longev 2018:1714896. https://doi.org/10.1155/2018/1714896.

Zhang Y, Li CN, Jiang WD, Wu P, Liu Y, Kuang SY, et al. An emerging role of vitamin D₃ in amino acid absorption in different intestinal segments of on-growing grass carp (*Ctenopharyngodon idella*). Anim Nutr 2022;10:305–18. https://doi.org/10.1016/j.aninu.2022.05.004.

Zhang Y, Li CN, Jiang WD, Wu P, Liu Y, Kuang SY, et al. Vitamin D serves as a modulator of immune organs in grass carp (*Ctenopharyngodon idella*) infected with *Aeromonas hydrophila*. Aquaculture 2023;565:739144. https://doi.org/10.1016/j.aquaculture.2022.739144.

Zhong WJ, Gu BH, Gu Y, Groome LJ, Sun JX, Wang YP, et al. Activation of vitamin D receptor promotes VEGF and CuZn-SOD expression in endothelial cells. J Steroid Biochem Mol Biol 2014;140:56–62. https://doi.org/10.1016/j.jsbmb.2013.11.017.